Monthly Notices
of the
ROYAL ASTRONOMICAL SOCIETY

Mon. Not. R. Astron. Soc. **401,** 1521–1531 (2010) doi:10.1111/j.1365-2966.2009.15779.x

On the stellar masses of IRAC detected Lyman Break Galaxies at $z \sim 3$

G. E. Magdis,[1,2⋆] D. Rigopoulou,[1,3] J.-S. Huang[4] and G. G. Fazio[4]

[1]*Department of Physics, University of Oxford, Keble Road, Oxford OX1 3RH*
[2]*CEA Saclay/Service d'Astrophysique, CNRS F-91191 Gif-sur-Yvette Cedex, France*
[3]*Rutherford Appleton Laboratory, Chilton, Didcot OX11 0QX*
[4]*Harvard-Smithsonian Center for Astrophysics, 60 Garden Street, Cambridge, MA 02138, USA*

Accepted 2009 September 23. Received 2009 September 23; in original form 2009 May 5

ABSTRACT

We present results of a large survey of the mid-infrared (mid-IR) properties of 248 Lyman Break Galaxies (LBGs) with confirmed spectroscopic redshift using deep *Spitzer*/Infrared Array Camera (IRAC) observations in six cosmological fields. By combining the new mid-IR photometry with optical and near-infrared observations, we model the spectral energy distributions (SEDs) employing a revised version of the Bruzual and Charlot synthesis population code that incorporates a new treatment of the thermal-pulsating asymptotic giant branch phase (CB07). Our primary aim is to investigate the impact of the AGB phase in the stellar masses of the LBGs, and compare our new results with previous stellar mass estimates. We investigate the stellar mass of the LBG population as a whole and assess the benefits of adding longer wavelengths to estimates of stellar masses for high-redshift galaxies. Based on the new CB07 code, we find that the stellar masses of LBGs are smaller on an average by a factor of ∼1.4 compared to previous estimates. LBGs with 8 and/or 24 μm detections show higher masses ($M_* \sim 10^{11}\,\mathrm{M}_\odot$) than LBGs faint in the IRAC bands ($M_* \sim 10^{9}\,\mathrm{M}_\odot$). The ages of these massive LBGs are considerably higher than the rest of the population, indicating that they have been star forming for at least ∼1 Gyr. We also show how the addition of the IRAC bands improves the accuracy of the estimated stellar masses and reduced the scatter on the derived mass-to-light ratios. In particular, we present a tight correlation between the 8 μm IRAC band (rest-frame K for galaxies at $z \sim 3$) and the stellar mass. We calculate the number density of massive ($M_* > 10^{11}\,\mathrm{M}_\odot$) LBGs and find it to be $\Phi = (1.12 \pm 0.4) \times 10^{-5}\,\mathrm{Mpc}^{-3}$, ∼1.5 times lower than that found by previous studies. Finally, based on ultraviolet-corrected star formation rates (SFRs), we investigate the SFR–stellar mass correlation at $z \sim 3$, find it similar to the one observed at other redshifts and show that our data place the peak of the evolution of the specific SFR at $z \sim 3$.

Key words: Catalogues – galaxies: high-redshift – early Universe.

1 INTRODUCTION

Although there has been considerable progress in understanding galaxy formation and evolution, current theoretical models still suffer from several uncertainties. These uncertainties are mainly introduced by the parameters that are very difficult to constraint, such as the initial mass function (IMF), the action of feedback by supernovae and stellar winds and the chemical evolution. Given that theoretical guidance is so uncertain, direct empirical information is essential in driving the investigation. The detection and study of high-z galaxies can put constraints on the physical parameters, put the existing models to the test and guide us to a better and more accurate description of the early galaxies. To this end, recent surveys have come to play a central role in modern cosmology, revealing a wealth of $z \sim 2$–3 star-forming galaxies.

Among others, there are two efficient methods of detecting high-z galaxies. The first relies on submillimetre blank field observations using the Submillimetre Common-User Bolometer Array (SCUBA) on the James Clerk Maxwell Telescope (e.g. Hughes et al. 1998) or the Max Plank Millimetre Bolometer array (MAMBO; e.g. Bertoldi et al. 2000) revealing the population of the submillimetre galaxies (SMGs) at $z > 2$ (e.g. Chapman et al. 2000; Ivison et al. 2002; Smail et al. 2002). The second relies on colour selection criteria, selecting high-z galaxies with different characteristics. For instance, the BzK colour criterion introduced by Daddi et al. (2003) selects moderately aged and moderately obscured star-forming galaxies at $z \sim 2$ while the $J_s - K_s > 2.3$ criterion (Franx et al. 2003;

⋆E-mail: georgios.magdis@cea.fr

van Dokkum & Ellis 2003) detects both strongly obscured by dust high-z star-forming galaxies as well as massive/evolved systems. One of the most common methods in the last decade though, now comprising an impressive catalogue of thousands of galaxies at $z \sim 3$, has been the selection based on photometric redshift gained from observations of the 'Lyman Break' located at 912 Å in the spectrum of a star-forming galaxy. The Lyman Break Galaxy (LBG) selection method was pioneered by Steidel et al. (1996, 1999, 2000, 2003), but has also been used by many other groups (e.g. Madau et al. 1996; Pettini et al. 2001; Bunker et al. 2004; Ouchi et al. 2004a,b; Stanway et al. 2004).

Since their detection, LBGs have caught the attention of the scientific community, and a considerable amount of effort has been concentrated on investigating and understanding their nature. To this direction, several strategies have been employed, ranging from multiwavelength photometric observations [from X-rays (Nandra et al. 2002; Laird et al. 2006) to submm (Chapman et al. 2000; Ivison et al. 2005)] to optical and near-infrared spectroscopy (e.g. Steidel et al. 1996; Pettini et al. 2001; Erb et al. 2003; Shapley et al. 2003).

One way to derive the properties of the LBGs is by fitting the observed spectral energy distribution (SED) with model SEDs, generated by stellar synthesis population codes. This technique was first applied by Sawicki & Yee (1998) to a sample of 17 LBGs from the *Hubble* Deep Field-North (HDF-N) (Williams et al. 1996). Later it was further employed by Papovich, Dickinson & Ferguson (2001) and Shapley et al. (2001) with NIR (rest-frame optical) photometry. Both groups derive similar stellar masses $\sim 10^{10}\,\mathrm{M}_{\odot}$ and agree that the stellar mass is generally well constrained by the fitting procedure in contrast to star formation rate (SFR) and stellar age which suffer from large uncertainties. Any study based only on rest-frame ultraviolet (UV)/optical data though, is far from complete, as the UV light of these galaxies samples only the short-lived massive stars of the forming populations. For a more comprehensive study, rest-frame near-infrared (near-IR) observations of galaxies are essential since they trace the bulk of the stellar emission. The advent of *Spitzer Space Telescope*, and its unprecedented sensitivity opened a window to the IR part of the spectrum of high galaxies and enabled the study of their infrared properties.

Up to date, there have been few mid-IR studies of LBGs. Using *Spitzer* observations, Barmby et al. (2004) investigated the properties of several hundred LBGs in Q1700, while Reddy et al. (2006), based on a sample of UV selected galaxies in HDF-N, found that they span 2 orders of magnitude in age and stellar mass and 4 orders of magnitude in dust obscuration. More recently, Shim et al. (2007) presented a study based on a sample of LBGs from a subregion of the First Look Survey. Although their sample lacks spectroscopic redshift they find that more than $\sim$70 per cent of the Infrared Array Camera (IRAC) detected LBGs have estimated stellar masses $>10^{11}\,\mathrm{M}_{\odot}$. A detailed mid-IR study of LBGs has been presented by Rigopoulou et al. (2006). Based on a sample of 175 LBGs with confirmed spectroscopic redshift in the Extended Groth Strip (EGS), they suggested that LBGs with bright IRAC colours are more massive ($M_{*} \sim 10^{11}\,\mathrm{M}_{\odot}$), older ($t_{\mathrm{sf}} \sim 1$ Gyr) and suffer more extinction when compared to the rest of the sample. Magdis et al. (2008), based on a sample of 751 LBGs, presented the mid-IR colours of LBGs and suggested that they are a rather inhomogeneous population ranging from those that have bright IRAC colours with SEDs that rise steeply towards longer wavelengths and $R - [3.6] > 1.5$ ('red' LBGs) to those that are faint in the IRAC bands with $R - [3.6] < 1.5$ ('blue' LBGs). Finally, Huang et al. (2005) reported the detection of several LBGs in the EGS at Multiband Imaging Photometer for SIRTF (MIPS) 24 μm, revealing a subset of LBGs, the infrared luminous LBGs (ILLBGs).

Despite those efforts, the mid-IR properties of the LBGs are not clear yet. Partially, this is due to that fact that the derived properties of the population depend critically on the adopted stellar synthesis population model. New developments of the stellar synthesis population codes, incorporating more accurate prescriptions of the stellar evolution phases and more particularly of the thermal-pulsating asymptotic giant branch phase (TP-AGB), allow us to derive more realistic and robust estimates of the properties of the population.

In this paper, we present mid-IR photometry for a sample of spectroscopically confirmed $z \sim 3$ LBGs detected as part of the IRAC Guaranteed Time Observations (GTO) program on six cosmological fields. Benefited from ground-based optical and IRAC observations, we are in the unique position to constrain the properties of the population. Although the stellar masses of the LBGs have been studied in the past, here we make use of a revised version of the Bruzual and Charlot stellar synthesis population code (CB07, private communication) that incorporates a new treatment of the TP-AGB phase and extend our study to explore the SFR–stellar mass relation at $z = 3$. Our aims are to investigate the impact of the new AGB-phase recipe on the stellar masses of the population, derive the range of the stellar masses of the LBGs and assess the benefits of adding longer wavelengths. In Section 2, we present a brief account of the observations and data reduction, while in Section 3 we describe the model parameters and the SED fitting of the observed SEDs, used to derive the properties of the population. Section 4 is dedicated to derived stellar masses. We quantify the impact of the addition of the AGB phase in the model SEDs, discuss the range of stellar masses of our sample and present the M/L as a function of wavelength. In Section 5, we focus on the number density of massive LBGs and present the stellar mass density (SMD) of our sample. Finally, in Section 6, we investigate the SFR–stellar mass correlation for star-forming galaxies at $z = 3$ while in Section 7 we summarize our results.

2 THE *SPITZER* LBG SAMPLE

The data for this study have been obtained with the (IRAC) (Fazio et al. 2004) on board the *Spitzer Space Telescope*. The majority of our data are part of the IRAC GTO program (PI G. Fazio) and include the fields: Q1422+2309 (Q1422), DSF2237a,b (DSF), Q2233+1341 (Q2233), SSA22a,b (SSA22) and B20902+34 (B0902) while data for the HDF-N come from the Great Observatories Origin Deep Survey program (GOODS, PI M. Dickinson). The data analysis and the mid-IR identification of the LBGs in these fields have been presented in detail by Magdis et al. (2008). Based on a catalogue of 1261 LBGs by Steidel et al. (2003) in these fields, we constructed a mid-IR sample of 751 LBGs, that were observed in at least one IRAC band. The sample consists of three categories of objects: those that have confirmed spectroscopic redshift (through follow up ground-based optical/NIR spectroscopy; Steidel et al. 2003) and are identified as galaxies at $z \sim 3$ (LBGs-z) or classified as active galactic nuclei (AGNs)/quasi-stellar object (QSO) and those that do not have spectroscopic redshift. In total, 321 LBGs-z, 12 AGN/QSO and 435 LBGs without spectroscopic redshift are covered. In Table 1, we list the ground based and IRAC photometry of LBGs-z from the current sample, that are observed in all IRAC bands.

In the current study, we focus on a subsample of 186 LBGs that (1) are observed in all IRAC bands, (2) are detected in at least one

Table 1. MIR photometric catalogue (*AB* magnitude) of LBGs with confirmed spectroscopic z. This is a sample of the full table, which is available in the online version of the article (see Supporting Information).

Name	z	U_n-G	G-R	R	3.6 μm	4.5 μm	5.8 μm	8.0 μm
B20902-C10	2.752	2.38	0.70	25.06	23.19 ± 0.19	23.20 ± 0.16	–	24.15 ± 0.50
B20902-C11	3.352	2.32	0.77	24.69	24.01 ± 0.41	–	–	–
B20902-C5	3.098	2.47	0.93	24.70	23.71 ± 0.36	22.99 ± 0.08	–	21.32 ± 0.09
B20902-C6	3.099	3.45	0.45	24.13	–	–	–	–
B20902-C7	3.195	3.16	0.37	24.52	–	24.13 ± 0.37	–	–
B20902-C8	2.970	2.90	0.76	24.40	–	–	–	–
B20902-C9	3.354	3.00	1.03	24.39	23.18 ± 0.19	22.93 ± 0.08	–	–
B20902-D11	2.835	1.81	0.29	22.97	21.71 ± 0.11	21.59 ± 0.09	–	21.20 ± 0.08
B20902-D14	2.766	2.20	0.59	24.40	22.38 ± 0.10	22.36 ± 0.11	–	23.53 ± 0.50
B20902-D8	2.867	1.80	0.24	24.24	23.52 ± 0.20	22.81 ± 0.08	–	–
B20902-D9	3.024	2.38	0.20	25.21	–	–	–	–
B20902-M11	3.303	2.65	1.18	24.19	23.00 ± 0.18	22.74 ± 0.10	–	–
B20902-M8	3.205	2.02	0.71	25.48	–	–	–	–
B20902-MD16	2.732	1.74	0.60	24.34	22.66 ± 0.09	–	–	22.71 ± 0.50

IRAC band, (3) have confirmed spectroscopic redshift (4) classified as galaxies, lacking a signature of strong AGN activity in their rest-UV spectrum (Shapley et al. 2003). In our sample, we add 10 LBGs that satisfy our criteria from the field Q1700.

Out of these, 71 LBGs are detected at 8 μm, consisting the 8 μm sample. As discussed by Magdis et al. (2008), whether a LBG is detected at 8 μm relies critically both on the depth of the observation and on how bright the LBG is in shorter wavelengths (i.e. 3.6 and 4.5 μm). Since in HDF-N, the deepest field of their study all LBGs with $[3.6]_{AB} < 23$ were detected at 8 μm, they extend the original 8 μm sample, by including the LBGs of shallower fields that were not detected at 8 μm but with $[3.6]_{AB} < 23$. We will refer to this as the 'extended 8 μm sample' and it consists of 105 LBGs. We also match our sample to the MIPS 24 μm catalogue of detected LBGs in HDF-N published by Reddy et al. (2006) (3σ, $f_{24} = 8$ μJy). Among the 8 μm detected LBGs in HDF-N, 18 LBGs are detected at 24 μm, while one of our galaxies (HDFN-M18) has $f_{24} = 88.2$ μJy and according to Huang et al. (2005) criterion is classified as a ILLBG ($f_{24} > 60$ μJy).

Although the current sample consists of LBGs lacking strong emission lines in their optical spectrum, one cannot rule out the presence of an obscured AGN. This issue was discussed by Magdis et al. (2008), where they showed that the mid-IR colours of the LBGs are consistent with that of star-forming galaxies and that AGNs at $z \sim 3$ tend to have brighter 8 μm fluxes and exhibit redder [4.5] − [8.0] colours. Another way to explore this possibility would be to search for object whose mid-IR SED is well fitted with a power law ($f_\nu \propto \nu^\alpha$ with $\alpha \leq -0.5$; Donley et al. 2007; Alonso-Herrero et al. 2006), indicative of the presence of hot dust heated by an AGN. However, the power-law galaxy selection using IRAC photometric points is not applicable at the redshift range of our sample. At $z \sim 3$, the IRAC bands sample the blue part of the 1.6 μm bump, dominated by light from the stellar component of a galaxy. Hence, even if an AGN exists, one cannot trace its signature at the wavelength range of 0.9–2 μm rest frame. This has also been pointed out by Donley et al. (2008), where they showed that at $z > 2.5$ the star-forming galaxy templates have IRAC SEDs that meet the typical power-law galaxy criteria. We note, however, that according to table 5 of Magdis et al. (2008), the fraction of AGN among the 8 μm detected LBGs is ∼11 per cent, compared to ∼3.5 per cent among the whole sample of $R < 25.5$ LBGs. Finally, the mean redshift of our sample is 2.92 (the distribution has $\sigma = 0.12$).

3 DERIVATION OF PHYSICAL PROPERTIES

We derive stellar masses for the LBG sample by fitting the latest CB07 stellar population synthesis models to the observed SEDs. The most important update of CB07 when compared to its predecessor (BC03) is the use of variable molecular opacities instead of the scaled-solar tables. Also, the calibration is not only based on the reproduction of the C-star luminosity function in both Magellanic Clouds, but also on the data for C- and M-star counts in Magellanic Cloud clusters, providing the right luminosities of the TP-AGB phase and the right contribution of TP-AGB stars to the integrated light (Marigo & Girardi 2007). In this section, we first describe the CB07 models and the fitting process that we use to infer the stellar masses and then comment on the uncertainties introduced by this type of analysis.

3.1 SED fitting

We use the CB07 code to generate model SEDs in order to fit the observed SEDs of 196 LBGs with confirmed spectroscopic redshift and at least one IRAC detection. Our aim is to derive the properties of the population and more particularly the stellar masses. We adopted the Padova 1994 stellar evolution tracks and constructed models with solar metallicity (see discussion in Shapley et al. 2005) and a Chabrier IMF. We use the Calzetti et al. (2000) starburst attenuation law to simulate the extinction by dust. We have considered two simple single-component models: exponentially declining models of the form $\mathrm{SFR}(t) \propto \exp(-t/\tau)$ with e-folding times of $\tau = 0.05$, 0.1, 0.5, 1.0, 1.5, 2.0 and 5.0 Gyr and continuous star formation (CSF) models ($\tau = \infty$).

Our model fitting followed standard procedures applied in similar studies of high-redshift galaxies (e.g. Papovich et al. 2001; Shapley et al. 2001; Forster Schreiber et al. 2004; Shapley et al. 2005; Papovich et al. 2006). The free parameters of our models are: dust extinction [$E(B-V)$], age ($t_{\rm sf}$ defining the onset of star formation), stellar mass (M_*), star formation (SFR) and star formation history (τ). For each of the star formation histories, we generated models with ages ranging from 1 Myr to the age of the Universe at the redshift of the galaxy being modelled, while we allowed the dust extinction to vary between $E(B-V) = 0$ and $E(B-V) = 1.0$. Furthermore, we computed the absorption by the intergalactic medium of neutral hydrogen (Madau 1995) at the

redshift of each galaxy, and attenuated appropriately the SED of the generated models. The model SEDs were then placed at the redshift of each galaxy and were compared to the observed SEDs by computing a reduced χ^2. The CB07 spectra are normalized to an SFR of $1\,M_\odot\ yr^{-1}$ for the CSF model while for the exponentially decaying models, the galaxy mass is normalized to $1\,M_\odot$ as $t = \infty$. For each individual galaxy, best-fitting parameters [age, $E(B-V)$ and normalizations] were derived from minimization of the reduced χ^2. This normalizations were then converted to best-fitting stellar mass and along with the best-fitting age, $E(B-V)$ and τ were considered the overall 'best fit'.

To quantify the error in the derived stellar masses, we compute the range of normalizations that result in an SED with reduced χ^2 values within $\Delta\chi^2_{\rm reduced} = 1$ of the minimum value. We adopt these as the 1σ uncertainties associated with the stellar masses. Finally, to facilitate comparisons with previous studies in the fields as well as to quantify the impact of the AGB phase on the derived stellar masses, we choose to repeat our analysis using this time models generated with BC03.

3.2 Model parameters and systematic uncertainties

Of course, the derived best-fitting parameters are subject to the adopted parameters of the model fits. In what follows we discuss how varying those properties affects the best-fitting SED parameters and uncertainties involved in this kind of analysis.

3.2.1 Extinction

The impact of different extinction laws has already been investigated by, for example, Papovich et al. (2001) and Dickinson et al. (2003), who found the effect to be overall small. For the present work, we have adopted the Calzetti et al. (2000) law. Such a law reproduces the total SFR from the observed UV for the vast majority of LBGs and accurately predicts the average X-ray and radio continuum fluxes of $z \sim 2$ star-forming galaxies (e.g. Nandra et al. 2002; Reddy & Steidel 2004; Reddy et al. 2005). The choice of the Calzetti law was also dictated by the desire to facilitate comparison with previous works in the field.

3.2.2 Metallicity and initial mass function

So far, information on element abundances in LBGs is rather limited. Pettini et al. (2002) determined element abundances in cB58, a typical L_* galaxy which benefits from a factor of 30 magnification, and found it to be $\sim 0.25\,Z_\odot$. Nagamine et al. (2001) suggested that near-solar metallicities are in fact common in $z \sim 3$ galaxies with masses greater than $10^{10}\,M_\odot$, which is broadly consistent with the results for cB58. Erb et al. (2006a) and Shapley et al. (2004) also argued for solar metallicities for $z \sim 3$ LBGs. Based on these results, we used solar metallicity in the models. Reducing metallicity to half solar would decrease the derived masses by 10–20 per cent (Papovich et al. 2001).

Finally, although the issue of the IMF that best describes the stellar population of high-z galaxies still remains open (e.g. Renzini et al. 2005; van Dokkum & van der Marel 2007; Dave 2008), recent results favour the scenario of a top-heavy IMF (e.g. Baugh et al. 2005; Nagashima et al. 2005; Lacey et al. 2008). Driven from these results we chose to use a Chabrier IMF to generate the CB07 models.

3.2.3 Systematic uncertainties

The systematic uncertainties, inherent in population synthesis modelling, have been studied and extensively described in the literature (e.g. Papovich et al. 2001; Shapley et al. 2001, 2005). The limitations of this technique mainly originate from the fact that the models cannot fully constrain the star formation history of high-z galaxies. In brief, the strong dependency of the inferred extinction and the age to the adopted star formation history introduces large degeneracies and makes the determination of these parameters highly uncertain.

These uncertainties are of course likely to affect the inferred stellar masses but in a less dramatic way. To test the impact of the adopted star formation history in the derived stellar masses it is worth comparing the inferred stellar mass of each galaxy for the two adopted star formation histories, namely constant (CSF) and exponentially decaying (EXP) star formation. We find that the agreement in the masses of individual objects is excellent, within the errors, with no obvious systematic trend or offset, indicating that the derived masses are robust and the adopted star formation history has a negligible effect on them ($\langle M_{*\rm CSF}\rangle = 10.471 \pm 0.101$ and $\langle M_{*\rm EXP}\rangle = 10.451 \pm 0.126$).

We note, however, that the uncertainties in the mass estimates become more serious when one assumes more complex star formation histories, such as the superposition of a young, roughly continuous episode of star formation and an old burst, with $t_{\rm sf} \gg \tau$, that peaked sometime in the past (Papovich et al. 2001) or introducing random bursts during the adopted star formation histories (Glazebrook, Abraham & McCarthy 2004). These studies indicate that the use of the simple star formation histories (CSF or EXP) is likely to provide a lower limit on the stellar mass estimate (Shapley et al. 2005).

4 THE STELLAR MASSES OF $Z \sim 3$ LBGS

Based on the best-fitting CB07 models, we derive the stellar masses of our sample population. The stellar masses, ages ($t_{\rm SFR}$) and extinction [$E(B-V)$] that correspond to the best-fitting models are listed in Table 2. Before examining the results though, we investigate the impact of the TP-AGB phase on the derived masses by

Table 2. CB07 best-fitting stellar population parameters. This is a sample of the full table, which is available in the online version of the article (see Supporting Information).

Name[a]	M^* ($10^9\,M_\odot$)	Age (Myr)	$E(B-V)$
B20902-C10	10.394 ± 0.115	101	1.566
B20902-C11	10.384 ± 0.086	9	0.589
B20902-C5	10.943 ± 0.078	1250	0.005
B20902-C7	9.529 ± 0.143	30	0.202
B20902-C9	10.641 ± 0.161	404	0.478
B20902-D11	11.175 ± 0.090	1434	0.138
B20902-D14	10.709 ± 0.136	71	1.566
B20902-D8	10.526 ± 0.101	1434	0.013
B20902-M11	10.721 ± 0.078	625	0.159
B20902-MD16	10.549 ± 0.114	508	0.689

[a]We did not fit the stellar populations of galaxies that had no data longward of R band, had uncertain redshifts, or are identified as AGN/QSO from their optical spectra. We also do not present SED parameters for those galaxies with optical and IRAC photometry inconsistent with a simple stellar population (these sources had large $\chi^2 > 10$.

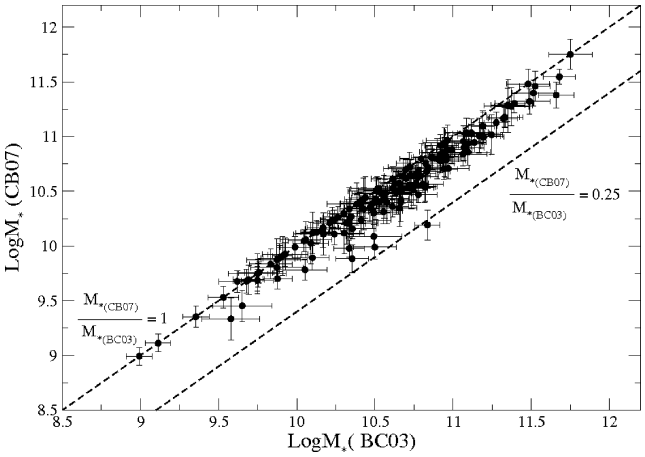

Figure 1. The derived best-fitting stellar masses for the whole sample of LBGs based on CB07 over those based on BC03. The black dashed lines correspond to $M_{*(CB07)}/M_{*(BC03)} = 1$ and $M_{*(CB07)}/M_{*(BC03)} = 0.25$, respectively.

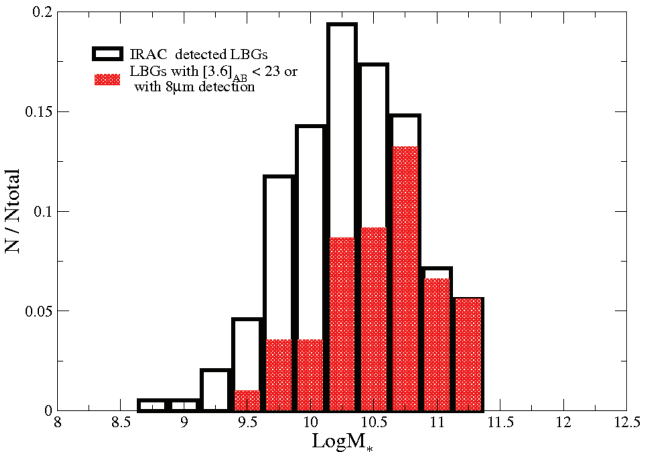

Figure 2. Distribution of the stellar masses derived from the best-fitting models for two samples: all LBGs with at least one IRAC detection (black) and LBGs with 8 μm detection or LBGs without 8 μm detection but with $[3.6]_{AB} < 23$ (red). The models assume a Chabrier IMF solar metallicity and the Calzetti et al. (2000) extinction law.

comparing the stellar masses obtained with CB07 and BC03 models, respectively.

4.1 The impact of the TP-AGB phase on the derived stellar masses

At a redshift of ∼3, the age of the universe is <2 Gyr, putting an upper limit in the age of those galaxies at 1–2 Gyr. As the AGB stars are of intermediate age (∼1 Gyr), one would expect to find such stars in the stellar content of $z \sim 3$ galaxies. If this is the case, since AGB stars are the dominant bolometric and near-IR contributors in stellar populations with ages ∼1 Gyr, the AGB-phase should be of great importance for the interpretation of the rest-frame near-IR *Spitzer* colours of these galaxies. Recent studies of $z \sim 2$ galaxies (e.g. Maraston et al. 2006; Eminian et al. 2008; Wuyts et al. 2007) have shown that incorporating the TP-AGB phase in the stellar synthesis population codes has resulted in the reduction of the estimated stellar masses and age by a factor of ∼2.

To investigate the impact of the new AGB recipe in the derive stellar masses of our sample, we compared the stellar masses derived from on CB07 model to those based on BC03 models. This comparison is illustrated in Fig. 1, where for each LBG we plot the stellar masses as derived from the best-fitting CB07 models over those derived based on BC03 ones. This figure clearly demonstrates that the masses based on BC03 models are consistently higher than those predicted by CB07. The mean stellar mass of the population is $\langle \log(M_*) \rangle = 10.621 \pm 0.106$ and 10.448 ± 0.099 for BC03 and CB07. This implies that the addition of the AGB phase results in the reduction of the derived stellar masses on average by 40 per cent for our whole IRAC detected sample. We note, however, that the reduction factor varies, and for some cases it can get as high as ∼3.

4.2 The stellar masses

As stated above, stellar mass is a robust parameter that is less sensitive to uncertainties compared to other parameters. In Magdis et al. (2008), we showed for the first time that LBGs are a rather inhomogeneous population, ranging from those with bright IRAC fluxes and $R - 3.6 > 1.5$ to those with $R - 3.6 < 1.5$ and marginal IRAC detection. Such diversity on the rest-frame optical colours of LBGs was also presented by Shapley et al. (2005). Here, we aim to translate this range in the IRAC colours into a range of the stellar masses. As stated above, stellar mass is a robust parameter that is less sensitive to uncertainties compared to other parameters. To visualize the stellar masses distribution of the population, in Fig. 2, we present a histogram of the inferred stellar masses for the whole *Spitzer* LBG sample and for LBGs with 8 μm detection or without 8 μm detection but $[3.6]_{AB} < 23$ (i.e. extended 8 μm sample).

The majority of the massive LBGs belong to the extended 8 μm sample which has a median stellar mass of $\log M_* = 10.711 \pm 0.105$, while for the rest LBGs the corresponding value is $\log M_* = 10.169 \pm 0.121$. In total, there are 62 LBGs with estimated stellar masses $M_* > 5 \times 10^{10}\,M_\odot$. Of these, 39 belong to the 8 μm sample, 51 to the extended 8 μm sample and only five to the remaining LBG sample. The same numbers for galaxies with $M_* > 10^{11}\,M_\odot$ are 21, 26 and 1, respectively. Splitting the 8 μm sample in two groups, those with $[8.0]_{AB} > 22.5$ and those with $[8.0]_{AB} < 22.5$ and performing a K–S test between the stellar masses of the two groups, reveals a significant difference between them ($P = 3.14 \times 10^{-7}$). In particular, we find that LBGs with bright 8 μm fluxes are more massive, with median stellar mass $\log M_* = 11.017 \pm 0.102$, compared to $\log M_* = 10.501 \pm 0.113$ for the 8 μm faint LBGs.

We now focus on 24 μm detected LBGs in HDF-N. These LBGs are also detected at 8 μm with a median 8 μm magnitude of $[8.0]_{AB} = 22.17 \pm 0.11$. The corresponding median 8 μm magnitude of the 24 μm undetected LBGs in HDF-N is $[8.0]_{AB} = 23.05 \pm 0.15$, indicating that they are on average fainter at 8 μm than the 24 μm detected LBGs. A Kolmogorov–Smirnov (K–S) test between the 8 μm magnitude distributions of the two samples confirms the significant difference between them at a confidence level of 98 per cent ($P = 0.021$). On the other hand, a second K–S test between the 8 μm fluxes of the 24 μm detected LBGs and the 24 μm undetected LBGs with $[8.0]_{AB} < 22.5$, reveals that the two samples are similar at a confidence level of 68 per cent, showing that 24 μm LBGs represent the bright end of the 8 μm sample. From the above analysis, it is expected that 24 μm LBGs are among the most massive galaxies in our sample. Indeed, 24 μm LBGs have a median stellar mass of $\log M_* = 10.901 \pm 0.109$, while the 24 μm undetected LBGs are less massive, with median, $\log M_* = 10.396 \pm 0.101$.

As discussed above, the age-dust degeneracy makes the parametrization of these two properties uncertain and difficult to constrain. With this in mind, it is worth noting that all LBGs with derived ages $t_{SFR} > 160$ Myr belong to the extended 8 μm sample. Furthermore, the median age of the 8 μm undetected, the 8 μm faint ($[8.0]_{AB} > 22.5$) and 8 μm bright ($[8.0]_{AB} < 22.5$) LBGs are 255.00, 404.154 and 980 Myr, respectively. Finally, if we restrict our sample to LBGs with comparable t_{SFR}, we find that those in the extended 8 μm sample are consistently more massive than those with IRAC faint colours. Since, in the same time interval, LBGs with 8 μm detection or $[3.6]_{AB} < 23$ have grown significantly larger stellar masses, we suggest that they are among the highest star-forming LBGs or that they have undergone more intensive star formation episodes than the rest LBGs. We note that although the current data cannot rule out in a definitive way that the 24 μm emission of these systems originates from the hot dust heated by an AGN, the lack of AGN signature in their rest-frame UV spectra as well as their SED, that resembles cold SCUBA sources (Huang et al. 2005), suggests that they are dominated by star formation.

Bringing these results together, we find that LBGs with bright IRAC fluxes are more massive and older when compared to the rest of the sample. This analysis has also revealed that although the addition of the AGB-phase has reduced the estimated stellar masses of LBGs, a substantial fraction of LBGs is still found to be massive with $M_* > 5 \times 10^{10}\,M_\odot$. LBGs with 8 μm detection are among the most massive in the present sample, while at the high end of the stellar mass distribution of the population we find LBGs with MIPS 24 μm emission.

This range in the stellar masses of the LBGs has also been reported in previous studies (e.g. Papovich et al. 2001; Shapley et al. 2001; Reddy et al. 2006; Rigopoulou et al. 2006). These studies, however, were based on SSP codes without a sophisticated treatment of the AGB-phase, namely using BC03. A direct comparison with our results indicates that these studies have overestimated the stellar masses of the LBGs by a factor of 1.5–2. For example, Rigopoulou et al. (2006) reports a median stellar mass for the 8 μm detected LBGs of $M_* = 10.98 \pm 0.112$, ∼1.8 times higher than that found in our study. Hence, it becomes apparent that a fraction of the rest-frame NIR light that was previously attributed to a number of relatively old stars (BC03) is now (CB07) interpreted as light emitted from stars in the AGB phase, resulting in the reduction of the derived stellar mass. We conclude that although the addition of the AGB-phase has not narrowed the range of the stellar masses of the LBGs, it has reduced the stellar mass budget of the population and to a greater extend of all star-forming galaxies older than 0.1 Gyr.

4.3 Mass-to-light ratios as a function of wavelength

It has been suggested that estimates of stellar mass from photometric measurements become increasingly reliable as one obtains longer wavelength data (e.g. Labbe et al. 2005), and that the addition of longer wavelength photometric points (i.e. the IRAC bands) plays a key role in our understanding of the properties of the LBG population as a whole. Here, we investigate the distribution of stellar mass with rest-frame wavelength as we move from optical to the near-infrared bands.

In Fig. 3 (top), we show the distribution of stellar masses for all IRAC detected LBGs, as a function of absolute [3.6] μm magnitude which at the median redshift of ∼3 corresponds to rest-frame 0.9 μm (i.e. *I* band). There is clearly a correlation between absolute *I*-band magnitude and stellar mass (correlation coefficient $r = 0.74$), while

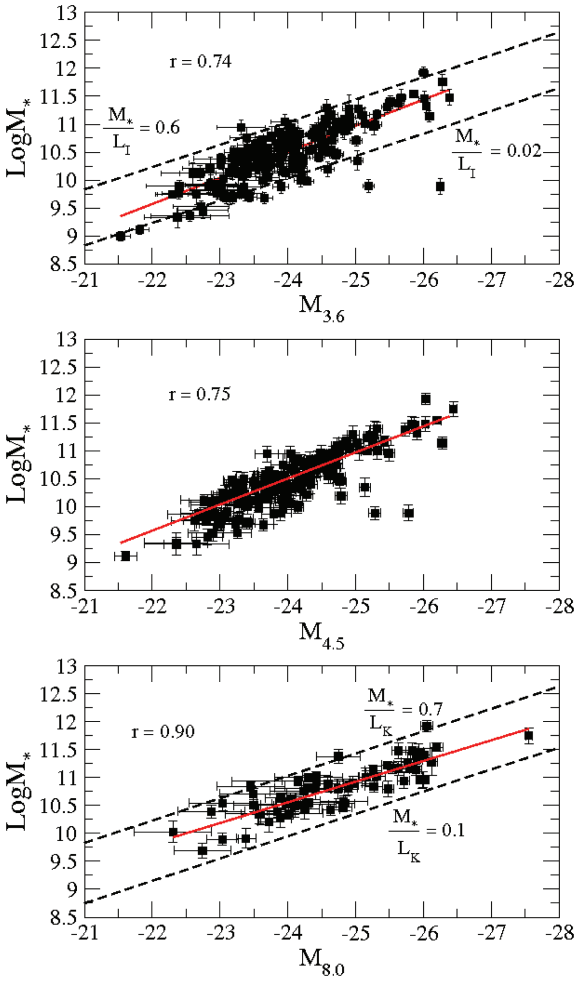

Figure 3. Stellar masses estimated from the best-fitting model (for all IRAC detected LBGs) as a function of absolute [3.6] μm magnitude, rest-frame *I* band (top), absolute $[4.5]_{AB}$ magnitude (middle) and absolute $[8.0]_{AB}$. The scatter in stellar mass-to-light ratio at a given 3.6 μm luminosity (rest-frame *I*-band luminosity at redshift 3) can be as high as 30 while at 8.0 μm (rest-frame K) it is significantly reduced. The dashed lines in the top and bottom panels indicate the range of stellar M/L in the sample and are given in solar units evaluated at rest-frame *I* and *K* bands while the red solid lines to the best linear regression fit. The *r* value for each regression is also noted.

at the bright end (where most of the massive galaxies are found) the correlation becomes tighter ($r = 0.90$, if we exclude the outlier). The M/L_I values (both M and L normalized in solar units) range from 0.6 [∼5 times lower than that of the present-day galaxies (Bell et al. 2003)] to 0.02, revealing a scatter of ∼30.

The spread in the M/L_I values can be attributed to the wide range of star-formation histories among the LBGs and it is therefore rather difficult to associate a single *I*-band rest-frame luminosity to specific a stellar mass. The situation remains the same at 4.5 μm as shown in Fig. 3 (middle panel).

Likewise, in Fig. 3 bottom panel, we plot the distribution of stellar masses as a function of absolute 8.0 μm magnitude which would correspond to rest-frame ∼2.0 μm (i.e. *K* band). The correlation between stellar mass and magnitude becomes tighter with $r = 0.90$ while the scatter in M/L_K values decreases and is now a factor of ∼7.0. The largest M/L_K values approach that of the present-day galaxies, but the average is 0.23, that is several times smaller. Due to

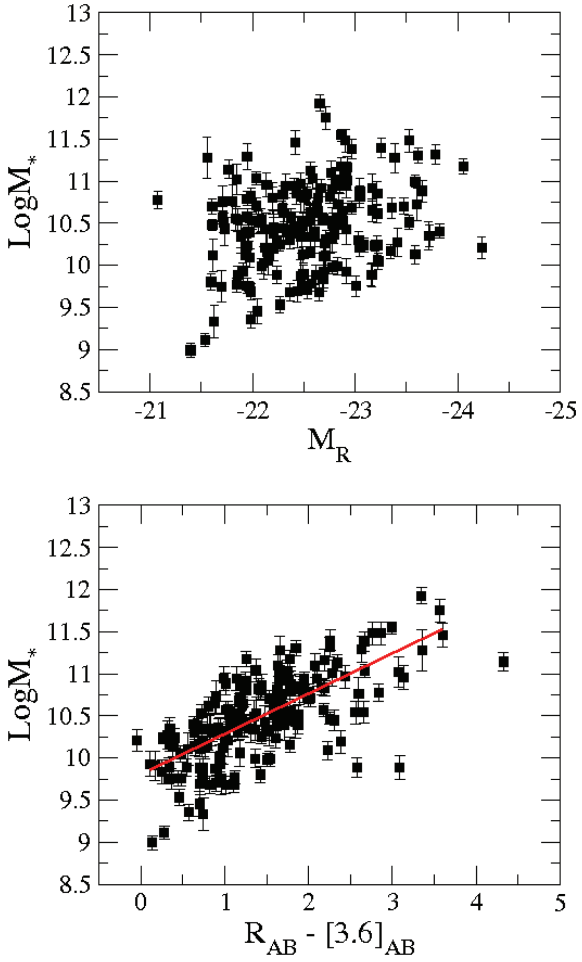

Figure 4. Top: stellar masses estimated from the best-fitting model as a function of absolute R magnitude. Bottom: stellar masses estimated from the best-fitting model as a function of $R - [3.6]_{AB}$ colour for LBGs in our sample. There is a strong correlation between masses and the $R - [3.6_{AB}]$ colour, particularly for the 8 μm LBG sample. The most massive objects ($M_* > 5 \times 10^{10}\,M_\odot$) tend to show the reddest $R - [3.6]_{AB}$ colours as well. The red line corresponds to the best linear regression fit.

the small scatter in the M/L values of the LBGs with 8 μm detection, one can crudely associate a K-band rest-frame absolute magnitude to a specific stellar mass through the relation:

$$\mathrm{Log}(M_*/\mathrm{M}_\odot) = 2.01(\pm 0.65) - 0.35(\pm 0.03) \times M_{8.0}.$$

From these simple comparisons, one can conclude that the mid-IR bands and especially the IRAC 8 μm band (which samples the rest frame NIR wavelengths for $z \sim 3$ LBGs) provide a more accurate estimate of the mass-to-light (M/L) ratio compared to that obtained when using optical bands. To further illustrate this argument, in Fig. 4 (top panel), we plot the distribution of stellar mass as a function of absolute R-band magnitude, for all LBGs in the present sample with at least one IRAC detection. The correlation coefficient drops to 0.32 and a mass-to-light relation cannot be established using only optical photometric points as the scatter in the M/L values is very large (possibly due to different star formation histories). With the addition of IRAC data this scatter decreases and is best correlated with the IRAC 8 μm band. This was somewhat expected since this band is sensitive to the light from the bulk of the stellar activity accumulated over the galaxy's lifetime (see also Bell & de Jong 2001).

The region of the spectrum that becomes sensitive to the ratio between the current star formation and the integral of past star formation, is between the UV and the NIR, conveniently measured by the observed $R - [3.6]_{AB}$ colour in the current sample. This point is illustrated in Fig. 4 (bottom panel), which shows that the inferred stellar mass is well correlated with $R - [3.6]_{AB}$. In fact, the correlation between the $R - [3.6]_{AB}$ colour and the inferred stellar mass is almost as significant as the correlation between stellar mass and $M_{4.5\,\mu\mathrm{m}}$, with LBGs with redder $R - [3.6_{AB}]$ colours having higher stellar masses. Finally, we note that in the high end of the stellar distribution one can find only LBGs that belong to the extended 8 μm sample. It is the bright IRAC colours that disentangle between the several star formation histories and provide a robust estimate of the mass to light ratios. Finally, 'red' LBGs with faint IRAC colours and hence low stellar masses could exist and occupy the bottom-right corner of Fig. 4 but are not present in the current sample due to the limiting apparent R magnitude (∼25.5) of their selection.

5 NUMBER DENSITY OF MASSIVE LBGS

It is interesting to find that, even after the addition of the AGB-phase, the best-fitting CB07 results indicate that ∼15 per cent of the LBGs in the present sample has estimated stellar masses ($M_* > 10^{11}\,\mathrm{M}_\odot$). These galaxies are mainly found among the LBGs that have IRAC 8 μm detection, consisting an ideal sample of high-z K-selected galaxies. In Fig. 5, we plot the number density of massive ($M_* > 10^{11}\,\mathrm{M}_\odot$) LBGs in our sample as a function of redshift and compare the value with other observational results (Saracco et al. 2004; Tecza et al. 2004; Drory et al. 2005; Fontana et al. 2006; Rigopoulou et al. 2006; Van Dokkum 2006; Shim et al. 2007). If we assume an effective volume for the U-dropouts $V = 450\ h^{-3}\,\mathrm{Mpc}^3\ \mathrm{arcmin}^{-2}$ (Steidel et al. 1999), the effective co-moving volume becomes $V = 1400\,\mathrm{Mpc}^3\ \mathrm{arcmin}^{-2}$ (the volumes have been weighted according to the number of objects per R-magnitude bin, $\Omega_\mathrm{m} = 0.3$, $\Omega_\lambda = 0.7$ cosmology with $H_0 = 70$ km $\mathrm{s}^{-1}\,\mathrm{Mpc}^{-1}$). For the LBGs with $M_* > 10^{11}\,\mathrm{M}_\odot$ in the 1066 arcmin^2 covered by our study, the derived comoving density at the average redshift $z \sim 3$ is $\Phi = (1.12 \pm 0.4) \times 10^{-5}\,\mathrm{Mpc}^{-3}$ (the uncertainty of the derived number density is based on Poisson error). This value is lower by a factor of ∼1.5 when compared to that found when we consider stellar masses derived from BC03 models ($1.67 \pm 0.32 \times 10^{-5}\,\mathrm{Mpc}^{-3}$). It is worth noting that our BC03 result is in excellent agreement with that of Rigopoulou et al. (2006) for a sample of 148 LBG in EGS. On the other hand, for the LBGs with $M_* > 8 \times 10^{10}\,\mathrm{M}_\odot$, we derive a comoving density of $\Phi = (1.75 \pm 0.26) \times 10^{-5}\,\mathrm{Mpc}^{-3}$ comparable to that of the BC03 result for LBGs with $M_* > 10^{11}\,\mathrm{M}_\odot$.

We have to stress that due to the spectroscopic selection of the LBGs in the present sample, we are restricted to optically bright (or rest-frame UV bright) LBGs ($R \leq 25.5$). Therefore, our sample does not account for the optically faint ($R > 25.5$) LBGs as well as for other optically faint massive populations at $z \sim 3$, such as distant red galaxies (DRGs) and SMGs. Reddy & Steidel (2009) found that the fraction of massive galaxies among UV-faint galaxies in general is very small (2 per cent) given the steep faint-end slope of the UV luminosity function. On the other hand, Van Dokkum (2006) suggest that 77 per cent of the massive galaxies at $2 < z < 3$ are selected as DRGs and 20 per cent as UV-bright LBGs. Furthermore, Tecza et al. (2004) report a number density of $8.9 \times 10^{-6}\,\mathrm{Mpc}^{-3}$ for massive SMGs, given that the overlap between LBGs and the rest of the populations is small between DRGs and LBGs ∼7 per cent (Van

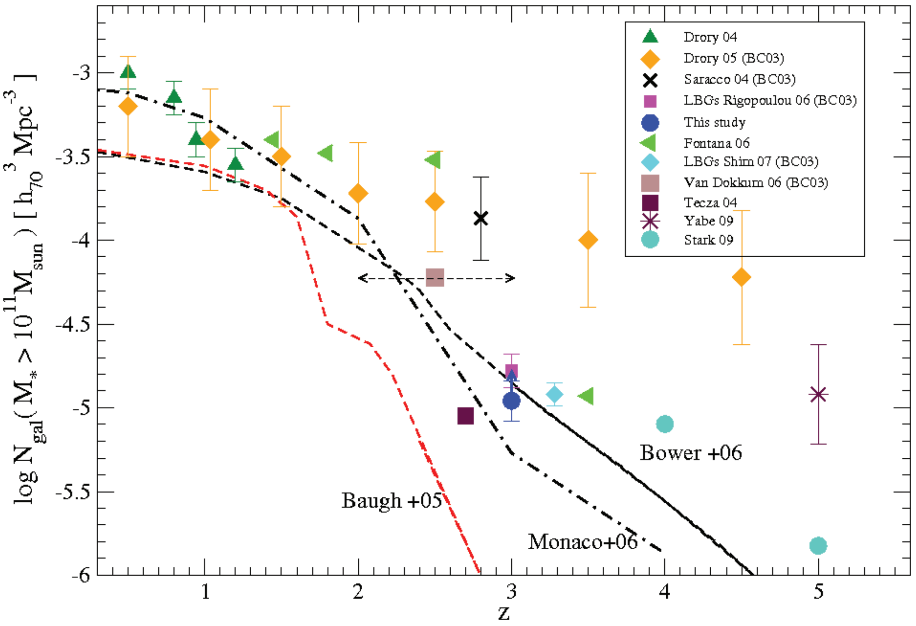

Figure 5. The number density of galaxies with stellar masses $>10^{11}\,M_{\odot}$ as a function of redshift. The blue filled circle shows our result for massive LBGs, while the blue box the result of massive LBGs by Rigopoulou et al. (2006). Data points from other observations are plotted with different symbols, and the prediction from recent semi-analytic and hydrodynamic models of galaxy formation are overplotted (red-dashed line from Baugh et al. 2005, black-dashed line for Bower et al. 2006, black-dashed–dotted line for Monaco et al. 2007).

Dokkum 2006 while between LBGs and SMGs is probably larger, ∼15 per cent Chapman et al. 2005), we note that the above number density of massive LBGs should be regarded as a lower limit for massive galaxies at $z \sim 3$. Despite the biases introduced by different selection techniques, LBGs constitute the largest existing sample of star-forming galaxies at $z \sim 3$ with confirmed spectroscopic redshift and therefore, our result places a firm and robust lower limit on the number density of massive galaxies at $z \sim 3$.

It is also worth comparing the present result with several theoretical predictions from semi-analytical models. In Fig. 5, it is evident that for the case of Baugh et al. (2005) the evolution of the number density of massive ($M_* \sim 10^{11}\,M_{\odot}$) galaxies with redshift is slower than the prediction of hierarchical models, at least in the redshift range $0 < z < 3$. On the other hand, the discrepancy between the model and the observational constraints is much reduced when one considers more recent predictions by Bower et al. (2006) and Monaco, Fontanot & Taffoni (2007). The galaxy formation model presented by Bower et al. (2006) is based on the hierarchical model of Cole et al. (2001). The key assumptions of this model are that at high z the cooling times in haloes were short enough to allow the gas to cool on the free-fall time-scale and that at the black hole masses were lower at high z. These two assumptions make the AGN feedback in their model less effective, allowing high-z massive galaxies to be built in the framework of the hierarchical model. We note that the fact that Bower et al. (2006) predictions exceed the number density of our sample is reasonable, since it allows for other massive galaxies, that are not selected with the Lyman Break technique, to exist at $z \sim 3$.

5.1 Stellar mass density of $z \sim 3$ LBGs

Determining the evolution of the global stellar mass with redshift is one of the most challenging tasks of modern cosmology. Hence, it would be interesting to estimate the SMD of our sample and attempt to place constraints on this property. Given the depth of our observations, our sample is completed at stellar masses $M_* > 2 \times 10^{10}\,M_{\odot}$. Therefore, we choose to integrate from $\log(M_*/M_{\odot}) = 10.301$ to $\log(M_*/M_{\odot}) = 13$ and derive a SMD $\rho = 7.08 \pm 0.8 \times 10^6\,M_{\odot}\,\mathrm{Mpc}^{-3}$. A comparison with the SMD at $z \sim 0.1$ as estimated by Cole et al. (2001) indicates that UV-bright LBGs with $M_* > 2 \times 10^{10}\,M_{\odot}$ at $z \sim 3$ harbour ∼2.5 per cent of the total stellar mass seen in the local universe. However, we have to stress that our sample is censored both at the high- and low-mass end. As discussed above, the Lyman Break selection technique misses ∼80 per cent of the massive galaxies at the redshift range $z = 2$– 3, although the actual fraction at $z = 3$ has not yet been quantified. On the other hand, focusing on the LBGs with IRAC detection introduces a bias against LBGs of lower stellar mass. Furthermore, as pointed out by Reddy & Steidel (2009), apart from the luminous and massive high-z galaxies, the faint-UV and less massive galaxies could also play an important role in the stellar mass assembly at these redshifts. More particularly, they claim that, for galaxies with $M_* < 10^{11}\,M_{\odot}$, the total stellar mass contained in UV faint is roughly equal to that contained in UV-bright galaxies. Hence, the above value is a lower limit not only for the whole $z \sim 3$ galaxies but also for the U-dropouts. Although we cannot make any safe assumptions about the fraction of massive LBGs and thus correct for the stellar masses residing in massive galaxies at $z \sim 3$, if we account for the contribution of the UV-faint galaxies to the stellar mass assembly, we find a SMD $\rho \sim 1.2 \times 10^7\,M_{\odot}\,\mathrm{Mpc}^{-3}$ for the UV selected galaxies at $z \sim 3$.

We now compare the SMD of our sample with that of other contemporary studies. In Fig. 6, we plot the evolution of the total SMD as a function of redshift for several samples drawn from the literature (Dickinson et al. 2003; Drory et al. 2005; Fontana et al. 2006; Rudnick et al. 2006; Elsner, Feulner & Hopp 2008; Perez-Gonzalez et al. 2008; Marchesini et al. 2009 (MUSYC); Eyles et al. 2007; Verma et al. 2007; Mancini et al. 2009). The values from the literature derived assuming a Salpeter (1955) IMF have been scaled to a pseudo-Chabrier IMF by dividing the stellar mass densities by a factor of 1.8. Although the values from the literature are either at lower or higher z than our sample, we note that our value is broadly

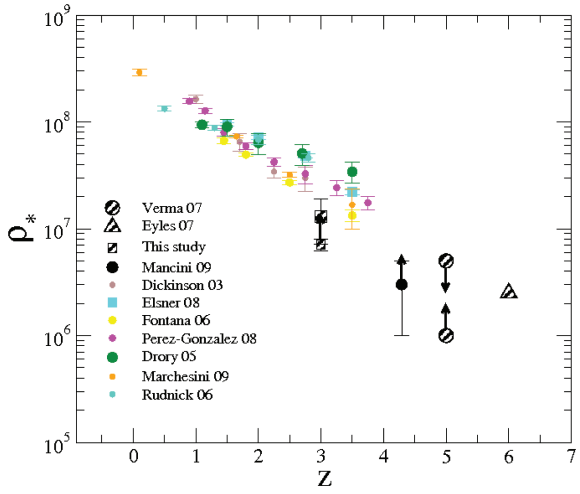

Figure 6. Evolution of the SMD with redshift. The *y*-axis indicates the SMD of galaxies at various redshifts, as estimated from several studies. Shadow-black symbols correspond to studies focused on LBGs. When necessary, values have been converted to a Chabrier IMF. For our study, we show the lower limit for UV-bright LBGs as well as the estimated ρ for the whole (bright + faint) UV-selected population of $z \sim 3$ galaxies (shadow-black boxes).

consistent with previous studies. The fact that, even after correcting for the contribution of faint-UV galaxies, our value is lower by a factor of ∼2 when compared to the general trend can be attributed to the stellar masses of optically faint massive galaxies (i.e. DRG, SMGs) and to systematics introduced by the different methods used to derive the stellar masses, especially the treatment of the AGB phase.

It is also interesting to compare our result with that of Verma et al. (2007), since the photometric criteria for selecting LBGs at $z \sim 5$ in their study were chosen to match that of Steidel et al. (2003) for our sample. It seems that LBGs at $z \sim 3$ have assembled 2–4 times more stellar mass than their high-z counterparts. We note again, that this type of analysis suffers from large uncertainties introduced by selection biases, cosmic variance and different methods of stellar mass determination, making it difficult to securely draw conclusions. On the other hand, LBGs at $z \sim 3$ consist of the largest existing sample of high-z galaxies with confirmed spectroscopic redshift, and hence their study provides robust constraints on the nature of high-z galaxies.

6 THE STAR FORMATION MASS CORRELATION AT $Z = 3$

Recently, Daddi et al. (2008) have shown that the UV-corrected SFR and stellar mass define a tight correlation in K-selected galaxies at $z \sim 2$. Similar results have been reached by Noeske et al. (2007) and Elbaz et al. (2007) for galaxies at $z \sim 1$ and at $z = 0$ based on data drawn from the Sloan Digital Sky Survey (Elbaz et al. 2007), although with a lower normalization reflecting the overall decline in cosmic SFR density with time (Madau et al. 1996). On the other hand, Daddi et al. (2009), based on an IRAC sample of B-dropouts, showed that the locus of typical massive $z \sim 4$ B-dropouts does not support a continuously increasing specific SFR (SSFR defined as the current SFR per unit stellar mass, ϕ) with redshift, suggesting instead a plateau of the SSFR at $z > 2$. Here, we try to fill the gap between $z = 2$ and 4, and examine the SFR-stellar mass relation at $z = 3$.

To determine the UV-corrected star-formation rate, we use the UV luminosity, assuming a CSF, Calzetti et al. (2000) extinction law and solar metallicity. At $z \sim 3$, the observed R and G bands correspond to rest-frame 1600 and 1200 Å respectively. We use these measurements to derive the β slope of the UV spectrum for each galaxy, after applying a correction for the IGM attenuation that follows the prescription of Madau (1995). Then, based on the best-fitting CB07 model SED derived as discussed in Section 3.1, we apply a K-correction to derive the observed flux at 1500 Å and a Calzetti et al. (2000) law to estimate the intrinsic L_{1500} for each galaxy in our sample. To convert the intrinsic L_{1500} to star-formation rate, we use the relation adopted by CB07 models,

$$\mathrm{SFR}(\mathrm{M}_{\odot}\,\mathrm{yr}^{-1}) = L_{1500\,\text{Å}}[\mathrm{erg\,s^{-1}\,Hz^{-1}}]/(8.85 \times 10^{27}). \quad (1)$$

Before going any further we have to stress that this technique suffers from several limitations. In applying a reddening correction, the technique assumes that the UV spectral slope is entirely due to reddening, rather than to the presence of evolved stellar populations. Furthermore, the strongest starbursts are opaque to UV radiation and their total SFR activity cannot thus be reliably estimated solely from the UV, even after reddening corrections (e.g. Goldader et al. 2002; Buat, Iglesias-Paramo & Seibert 2005; Reddy et al. 2006). On the other hand, Rigopoulou et al. (2006) argued that the fact that a fraction of LBGs is detected at 24 μm implies the existence of significant amounts of dust. This indicates that dust and not evolved stellar populations is responsible for the UV spectral slope, favouring a CSF history. Moreover, Carilli et al. (2008), based on stacking radio analysis of U-dropouts from the Cosmos field, found that the SFR implied by the radio luminosities are larger by a factor of ∼1.8 when compared to that derived from UV luminosities without correcting for dust extinction.

Finally, Chapman & Casey (2009) and Rigopoulou et al. (in preparation) using SCUBA and Institute for Radio Astronomy in the Millimeter Range observations both report on the detection of LBGs in submm. In particular, Chapman & Casey (2009) find a good agreement between UV and S_{850} derived SFR at faint submm levels and suggest that LBGs may contribute significantly to the source counts of submm selected galaxies in the 1–2 mJy regime. This indicates that considerable amounts of dust are found in LBGs. Evidence, that LBGs contain significant amounts of dust have also been provided by several other studies such as Papovich et al. (2001), Shapley et al. (2001) and Reddy et al. (2006). This, along with the fact that LBGs are (from their selection) blue actively star-forming galaxies, enforces the assumption of a UV spectrum reddened by the presence of dust rather than by a decaying SFR. Hence, the main source of uncertainty in our approach should be the adopted extinction law and the geometry of the distribution of the dust.

Having discussed the uncertainties, in Fig. 7, we show the SFR-stellar mass relation using the UV corrected SFRs and the stellar masses as estimated by our CB07 analysis assuming a CSF history. We restrict our sample to LBGs at $2.8 < z < 3.2$, detected at both 3.6 and 4.5 μm and $\Delta R < 0.2$ (where ΔR is the error of the R_{AB} magnitude) to reduce the uncertainty on the estimated β slope, and therefore the SFR. A linear regression fit to our data suggests a relatively tight correlation ($r = 0.70$) with a logarithmic slope ∼0.91 (although with considerable scatter), implying that more massive LBGs tend to have higher star-formation rates. The slope of this correlation is similar to that at lower redshifts (Elbaz et al. 2007; Noeske et al. 2007; Daddi et al. 2008) but with higher normalization factor. On the other hand, the current normalization factor is higher than that of the B-dropouts at $z \sim 4$. With a median SSFR, of

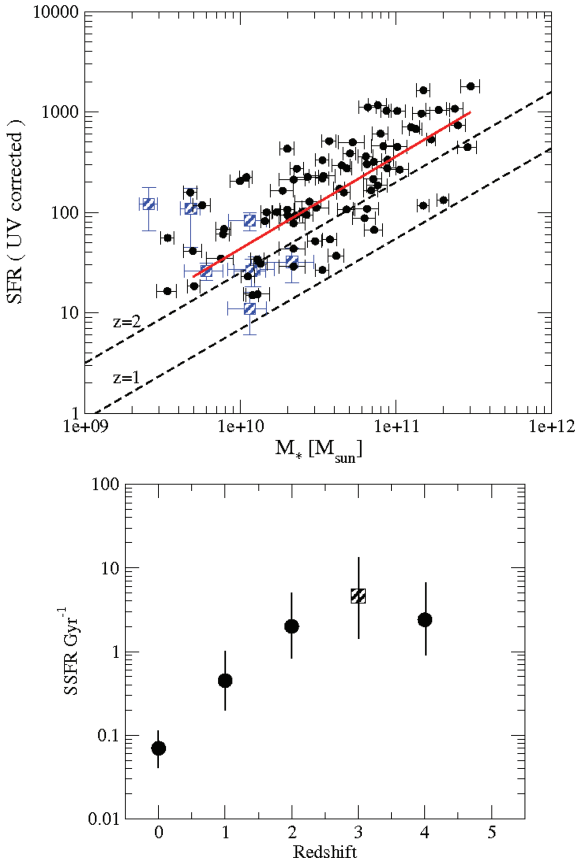

Figure 7. Upper: the UV-corrected SFR over the stellar masses for our sample. The red line corresponds to the linear regression best fit ($r = 0.70$) with a slope $\alpha = 0.91$. The black-dashed lines correspond to the SFR–$M_\star$ relation at $z = 2$ and 1 by Daddi et al. (2008) and Elbaz et al. (2007), respectively. Blue boxes correspond to Hβ based SFRs for LBGs at $z \sim 3$ by Mannucci et al. (2009). Bottom: specific star formation rate (SSFR = SFR/M$_\star$) as a function of redshift. Black circles show the average SSFR at a stellar mass of $5 \times 10^{10}\,M_\odot$ from Daddi et al. (2009) and Elbaz et al. (2007), while the black-shadowed box corresponds to the measurement of the current study for galaxies at $z = 3$. The vertical lines show the measured 1σ range.

$\sim$4.5 Gyr^{-1}, which is larger by a factor of 2 than that of $z \sim 2$ and $z \sim 4$ samples, it seems that the evolution of the SSFR peaks at $z \sim 3$ and then drops towards lower redshifts (Fig. 7, bottom).

Contrary to our findings, Mannucci et al. (2009), based on SFRs derived from Hβ fluxes of LBGs, argued that $z \sim 3$ LBGs do not show a correlation between SFR and stellar mass. To investigate this discrepancy, we include their results in Fig. 7 (top). We see that the small number as well as the small range of the stellar masses of the LBGs in their sample are not sufficient to reveal any correlation. As a matter of fact, their result is in agreement with ours for a small stellar mass bin. Indeed, if we restrict our sample to LBGs with $9 < \log M_*/M_\odot < 10.3$, the scatter in their sample is similar to the one we find, indicating that there is no correlation between SFR and stellar mass. It is the large numbers and the large stellar mass range of our sample that enables the detection of the correlation. A similar trend although with shallower slope is also reported by Erb et al. (2006a) for a sample of $z \sim 2$ UV selected galaxies. We conclude that although further investigation is required, the SFR–stellar mass relation seen in lower redshifts seems to hold for $z \sim 3$ LBGs. Finally, one should note that the average SFR found for our sample ($>100\,M_\odot$ yr^1) should be regarded as typical only for IRAC detected and hence more massive LBGs.

7 SUMMARY

Using IRAC photometry for a robust sample of 196 LBGs at $z \sim 3$ with confirmed spectroscopic redshift, we carried out a detailed mid-IR study of the LBG population. For our analysis, we used both the new CB07 code that incorporates an updated prescription of the AGB phase as well as the widely used BC03. The following results were reached.

(i) *Stellar masses.* Based on the results derived by the CB07 code, we constrained the properties of the population. We find that although the addition of the AGB phase has resulted in the reduction of the derived stellar masses, on average by a factor of $\sim$1.4, the range of the stellar masses of the LBGs is similar to that found by previous studies. In particular, we find that the stellar masses of the population span from $M_* \sim 10^9\,M_\odot$ for LBGs with faint IRAC colours to $M_* \sim 10^{11}\,M_\odot$ for a fraction of LBGs detected at 8 μm and for ILLBGs. The inferred ages of these massive systems are considerably higher than the rest of the population, indicating that they have been star forming for $\sim$1 Gyr. We show how the stellar mass correlates with wavelength and find that IRAC bands improve dramatically the accuracy of the derived M/L ratios when compared to that obtained when using optical bands. Finally, we show that LBGs with redder $R - [3.6]_{AB}$ colours have higher stellar masses.

(ii) *Number density and SMD of massive LBGs.* We find that even after the addition of the AGB phase in the SED models, a considerable fraction of LBGs ($\sim$15 per cent) is massive, with stellar masses $M_* > 10^{11}\,M_\odot$. We calculate the number density of these LBGs and find $\Phi = (1.12 \pm 0.4) \times 10^{-5}$ Mpc^{-3}. This is $\sim$1.5 times lower than that predicted from previous studies, providing a better match with current theoretical models. The SMD of IRAC detected, optically bright LBGs is $\rho = 7.08 \pm 0.8 \times 10^6\,M_\odot$ Mpc^{-3}, indicating a lower limit for the SMD of the whole UV selected population of $z = 3$ galaxies, $\rho \sim 1.2 \times 10^5\,M_\odot$ Mpc^{-3}. Comparing our result with values from the literature, we find that LBGs at $z = 3$ have assembled 2–4 times more stellar mass than their high-z siblings.

(iii) *Star-formation–mass correlation at $z = 3$.* We find a relatively tight correlation between the UV-corrected SFR and stellar mass for galaxies at $z = 3$. This correlation has a similar slope to that found at other redshifts, but a higher normalization factor. We find an average SSFR of 4.6 Gyr^{-1} for our sample, indicating that the evolution of the SSFR peaks at $z = 3$ and drops at lower redshifts.

ACKNOWLEDGMENTS

This work is based on observations made with the *Spitzer Space Telescope*, which is operated by the Jet Propulsion Laboratory, California Institute of Technology under a contract with NASA. Support for this work was provided by NASA through an award issued by JPL/Caltech. GEM would like to thank S. Charlot for providing the new CB07 code as well as D. Elbaz, H. Aussel and E. Daddi for useful discussions.

REFERENCES

Alonso-Herrero A. et al., 2006, ApJ, 640, 167
Barmby P. et al., 2004, ApJS, 154, 97
Baugh C. M., Lacey C. G., Frenk C. S., Granato G. L., Silva L., Bressan A., Benson A. J., Cole S., 2005, MNRAS, 356, 1191
Bell E. F., de Jong R. S., 2001, ApJ, 550, 212
Bell E. F., McIntosh D. H., Katz N., Weinberg M. D., 2003, ApJS, 149, 289
Bertoldi F. et al., 2000, A&A, 360, 92

Bower R. G., Benson A. J., Malbon R., Helly J. C., Frenk C. S., Baugh C. M., Cole S., Lacey C. G., 2006, MNRAS, 370, 645
Buat V., Iglesias-Paramo J., Seibert M., 2005, ApJ, 619, L51
Bunker A. J., Stanway E. R., Ellis R. S., McMahon R. G., 2004, MNRAS, 355, 374
Calzetti D., Armus L., Bohlin R. C., Kinney A. L., Koornneef J., Storchi-Bergmann T., 2000, ApJ, 533, 682
Carilli C. L. et al., 2008, ApJ, 689, 883
Chapman S. C., Casey C. M., 2009, MNRAS, 398, 1615
Chapman S. C. et al., 2000, MNRAS, 319, 318
Chapman S. C., Blain A. W., Smail I., Ivison R. J., 2005, ApJ, 622, 772
Cole S. et al., 2001, MNRAS, 326, 255
Daddi E. et al., 2003, ApJ, 588, 50
Daddi E., Dannerbauer H., Elbaz D., Dickinson M., Morrison G., Stern D., Ravindranath S., 2008, ApJ, 673, L21
Daddi E. et al., 2009, ApJ, 694, 1517
Dave R., 2008, MNRAS, 385, 147
Dickinson M., Papovich C., Ferguson H. C., Budavri T., 2003, ApJ, 587, 25
Donley J. L., Rieke G. H., Perez-Gonzalez P. G., Rigby J. R., Alonso-Herrero A., 2007, ApJ, 660, 167
Donley J. L., Rieke G. H., Perez-Gonzalez P. G., Barro G., 2008, ApJ, 687, 111
Drory N., Salvato M., Gabasch A., Bender R., Hopp U., Feulner G., Pannella M., 2005, ApJ, 619, L131
Elbaz D. et al., 2007, A&A, 468, 33
Elsner F., Feulner G., Hopp U., 2008, A&A, 477, 503
Eminian C., Kauffmann G., Charlot S., Wild V., Bruzual G., Rettura A., Loveday J., 2008, MNRAS, 384, 930
Erb D. K. et al., 2003, ApJ, 591, 101
Erb D. K., Shapley A. E., Pettini M., Steidel C. C., Reddy N. A., Adelberger K. L., 2006a, ApJ, 644, 813
Erb D. K., Steidel C. C., Shapley A. E., Pettini M., Reddy N. A., Adelberger K. L., 2006b, ApJ, 647, 128
Eyles L. P. et al., 2007, MNRAS, 374, 910
Fazio G. G. et al., 2004, ApJS, 154, 106
Fontana A. et al., 2006, A&A, 459, 745
Förster Schreiber N. M. et al., 2004, ApJ, 616, 40
Franx M. et al., 2003, ApJ, 587, L79
Glazebrook K., Abraham R. G., McCarthy P. J., 2004, Nat, 430, 181
Goldader J. D., Meurer G., Heckman T. M., Seibert M., Sanders D. B., Calzetti D., Steidel C. C., 2002, ApJ, 568, 651
Huang J.-S. et al., 2005, ApJ, 634, 137
Hughes D. H. et al., 1998, Nat, 394, 241
Ivison R. J. et al., 2002, MNRAS, 337, 1
Ivison R. J. et al., 2005, MNRAS, 364, 1025
Labbe I. et al., 2005, ApJ, 624, L81
Lacey C. G., Baugh C. M., Frenk C. S., Silva L., Granato G. L., Bressan A., 2008, MNRAS, 385, 1155
Laird E. S., Nandra K., Hobbs A., Steidel C. C., 2006, MNRAS, 373, L217
Madau P., 1995, ApJ, 441, 18
Madau P., Ferguson H. C., Dickinson M. E., Giavalisco M., Steidel C. C., Fruchter A., 1996, MNRAS, 283, 1388
Magdis G. E., Rigopoulou D., Huang J.-S., Fazio G. G., Willner S. P., Ashby M. L. N., 2008, MNRAS, 386, 11
Mancini C. et al., 2009, A&A, in press (arXiv:0901.3341)
Mannucci F. et al., 2009, MNRAS, in press (arXiv:0902.2398)
Maraston C. et al., 2006, ApJ, 652, 85
Marchesini D., van Dokkum P. G., Forster Schreiber N., Franx M., Labbe I., Wuyts S., 2009, ApJ, 701, 1765
Marigo P., Girardi L., 2007, A&A, 469, 239
Monaco P., Fontanot F., Taffoni G., 2007, MNRAS, 375, 1189
Nagamine K., Fukugita M., Cen R., Ostriker J. P., 2001, MNRAS, 327, L10
Nagashima M., Lacey C. G., Baugh C. M., Frenk C., Cole S., 2005, MNRAS, 358, 1247
Nandra K., Mushotzky R. F., Arnaud K., Steidel C. C., Adelberger K. L., Gardner J. P., Teplitz H. I., Windhorst R. A., 2002, ApJ, 576, 625
Noeske K. G. et al., 2007, ApJ, 660, L43
Ouchi M. et al., 2004a, ApJ, 611, 660
Ouchi M. et al., 2004b, ApJ, 611, 685
Papovich C., Dickinson M., Ferguson H., C., 2001, ApJ, 559, 620
Papovich C. et al., 2006, ApJ, 640, 92
Perez-Gonzalez P. G. et al., 2008, ApJ, 675, 234
Pettini M., Pagel B. E. J., 2004, MNRAS, 348, L59
Pettini M., Shapley A. E., Steidel C. C., Cuby J., Dickinson M., Moorwood A. F. M., Adelberger K. L., Giavalisco M., 2001, ApJ, 554, 981
Pettini M., Rix S. A., Steidel C. C., Adelberger K. L., Hunt M. P., Shapley A. E., 2002, ApJ, 569, 742
Reddy N. A., Steidel C. C., 2004, ApJ, 603, L13
Reddy N. A., Steidel C. C., 2009, ApJ, 692, 778
Reddy N. A., Erb D. K., Steidel C. C., Shapley A. E., Adelberger K. L., Pettini M., 2005, ApJ, 633, 748
Reddy N. A., Steidel C., Fadda D., Yan L., Pettini M., Shapley A. E., Erb D. K., Adelberger K. L., 2006, ApJ, 644, 792
Renzini A., Buzzoni A., 1986, in Chiosi C., Renzini A., eds, Spectral Evolution of Galaxies, Astrophys. Space Sci. Libr. Vol. 122. Reidel, Dordrecht, p. 195
Rigopoulou D. et al., 2006, ApJ, 648, 81
Rudnick G. et al., 2006, ApJ, 650, 624
Salpeter E. E., 1955, ApJ, 121, 161
Saracco P. et al., 2004, A&A, 420, 125
Sawicki M., Yee H. K. C., 1998, AJ, 115, 1329
Shapley A. E. et al., 2001, ApJ, 562, 95
Shapley A. E., Steidel C. C., Pettini M., Adelberger K. L., 2003, ApJ, 588, 65
Shapley A. E., Steidel C. C., Erb D. K., Reddy N. A., Adelberger K. L., Pettini M., Barmby P., Huang J., 2005, ApJ, 626, 698
Shim H., Im M., Choi P., Yan L., Storrie-Lombardi L., 2007, ApJ, 669, 749
Smail I., Ivison R. J., Blain A. W., Kneib J.-P., 2002, MNRAS, 331, 495
Stanway E. R., Bunker A. J., McMahon R. G., Ellis R. S., Treu T., McCarthy P. J., 2004, ApJ, 607, 704
Steidel C. C., Giavalisco M., Dickinson M., Adelberger K. L., 1996, AJ, 112, 352
Steidel C. C., Adelberger K. L., Giavalisco M., Dickinson M., Pettini M., 1999, ApJ, 519, 1
Steidel C. C., Adelberger K. L., Shapley A. E., Pettini M., Dickinson M., Giavalisco M., 2000, ApJ, 532, 170
Steidel C. C., Adelberger K. L., Shapley A. E., Pettini M., Dickinson M., Giavalisco M., 2003, ApJ, 592, 728
Tecza M. et al., 2004, ApJ, 605, L109
van Dokkum P. G., Ellis R. S., 2003, ApJ, 592, L53
van Dokkum P. G., 2006, ApJ, 638, L59
van Dokkum P. G., van der Marel R. P., 2007, ApJ, 655, 30
Verma A. et al., 2007, MNRAS, 377, 1024
Williams R. E. et al., 1996, AJ, 112, 1335
Wuyts S. et al., 2007, ApJ, 655, 51

SUPPORTING INFORMATION

Additional Supporting Information may be found in the online version of this article:

Table 1. MIR photometric catalogue (AB magnitude) of LBGs with confirmed spectroscopic *z*.
Table 2. CB07 best-fitting stellar population parameters.

Please note: Wiley-Blackwell are not responsible for the content or functionality of any supporting materials supplied by the authors. Any queries (other than missing material) should be directed to the corresponding author for the article.

This paper has been typeset from a TEX/LATEX file prepared by the author.